

A NOVEL EFFICIENT MULTI-VIEW TRAFFIC-RELATED OBJECT DETECTION FRAMEWORK

Kun Yang¹, Jing Liu¹, Dingkang Yang¹, Hanqi Wang¹, Peng Sun², Yanni Zhang³, Yan Liu⁴, Liang Song^{1,3*}

¹Academy for Engineering & Technology, Fudan University, China

²Duke Kunshan University, China

³Shanghai East-bund Research Institute on NSAI, China

⁴Jiangxi Open University, China

ABSTRACT

With the rapid development of intelligent transportation system applications, a tremendous amount of multi-view video data has emerged to enhance vehicle perception. However, performing video analytics efficiently by exploiting the spatial-temporal redundancy from video data remains challenging. Accordingly, we propose a novel traffic-related framework named CEVAS to achieve efficient object detection using multi-view video data. Briefly, a fine-grained input filtering policy is introduced to produce a reasonable region of interest from the captured images. Also, we design a sharing object manager to manage the information of objects with spatial redundancy and share their results with other vehicles. We further derive a content-aware model selection policy to select detection methods adaptively. Experimental results show that our framework significantly reduces response latency while achieving the same detection accuracy as the state-of-the-art methods.

Index Terms— Intelligent transportation system, cooperative perception, video analytics, edge intelligence

1. INTRODUCTION

Recently, video analytics-based applications have been widely applied to support smart cities, including traffic monitoring [1–3] and video surveillance [4, 5]. To improve the efficiency of video analysis, some studies [6, 7] explored temporal correlations in videos and assigned the region of interest (RoI) accordingly. For example, motion vector and optical flow are adopted to implement tracking methods in [8–10]. In [11], the authors proposed an LSTM-based model to predict the RoI. As for the multi-camera scenarios, many researchers exploited the physical correlations between cameras. For instance, in [4, 12], a location model was adopted to track target objects in a multi-camera network; Caesar [13] detected complex behaviors using the spatial-temporal correlations between surveillance cameras. Meanwhile, with the

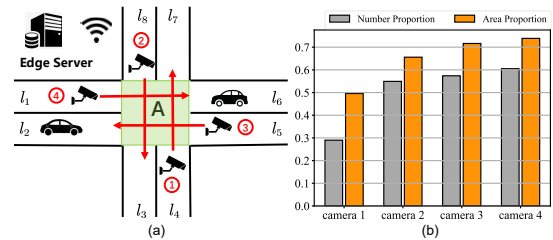


Fig. 1. Intersection and quantification of spatial redundancy.

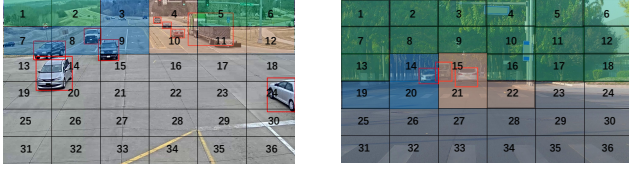
development of vehicle-to-everything (V2X) communication technology [14], the concept of cooperative perception [15–18] was proposed to improve the vehicles’ ability to perceive the system wide traffic conditions. Briefly, vehicles can share the self-acquired traffic information with other participants (e.g., other vehicles and traffic monitoring equipment). Different from the existing point cloud-based methods [19–23], we propose utilizing multi-view video data from different vehicles to achieve more efficient cooperative perception. We need to solve the following challenges.

Fig. 1(a) shows a common method for deploying cameras at intersections. Since all four cameras can capture the vehicles in the intersection (region A), the video information about region A is redundant for video analytics. Fig. 1(b) lists the number and area proportion of the vehicles located in the region A among all detectable vehicles. The results indicate that lots of redundant information exist in the multi-view video data due to the overlapping detection ranges of cameras, namely spatial redundancy. Moreover, considering that the correlations between consecutive frames produce another type of redundant information [24–26] (called temporal redundancy), a mechanism that can eliminate these two types of redundancy simultaneously is needed. The last challenge is related to computing efficiency. Since the content of each video frame varies, we need to select the detection methods (e.g., YOLO [27] and SSD [28]) adaptively rather than using a fixed detector.

To tackle the above challenges, we design a traffic-related object detection framework, CEVAS, to support video analytics-based cooperative perception. Summarily, we propose a fine-grained input filtering policy to produce the

* Corresponding author.

This work is partially supported by the Shanghai Key Research Laboratory of NSAI and NSFC Grant 62250410368.



(a) Traffic monitor. (b) Vehicular camera.
Fig. 2. The captured images of diverse agents.

RoI from images, which can eliminate the temporal redundancy between consecutive frames and the spatial redundancy across cameras. Also, we adopt the sharing object manager to manage the objects with spatial redundancy and guarantee the detection accuracy of each agent through result sharing. Further, a lightweight model selection policy is introduced to select detection methods adaptively.

2. SYSTEM MODEL

In this section, we will introduce our cooperative perception model and the corresponding region partitioning policy.

2.1. Cooperative Perception Model

We consider the cooperative perception model in Fig. 1(a). C_i denotes the i -th agent with cameras, including traffic monitors and vehicular cameras. The image captured by C_i at time t is denoted as F_t^i . Upon receiving F_t^i via wireless connections, the edge server detect the objects $\{O_{t,j}^i, O_{t,j'}^i\}$ via detection methods and return results D_t^i , which contains the corresponding bounding boxes (bboxes) $\{p_{t,j}^i, p_{t,j'}^i\}$.

2.2. Region Partitioning Policy

We first divide the whole image into multiple blocks with a fixed size and number them sequentially. Let b_k denote the blocks. Then, based on the location of the vehicles appearing in the picture and their driving direction, we divide the field of view of a camera into four regions as follows:

The blocks where vehicles will not appear are set as the *background region*, marked in green in Fig. 2. We define entrance lanes as the *incoming region* R_{in} and labeled as the blue blocks in Fig. 2. As the vehicles in R_{in} gradually approach the intersection, they will occupy more pixels and be detected, treated as **new objects**. In contrast, the exit lanes is defined as the *leaving region* R_l and labeled as orange blocks in Fig. 2. The vehicles in R_l will move away from the intersection and occupy fewer pixels. We consider the intersection (region A) as the overlapping region R_o , corresponding to the blocks without colors in Fig. 2. The vehicles in R_o are defined as **sharing objects**, which will be captured by multiple agents simultaneously despite the different driving states.

3. THE PROPOSED CEVAS FRAMEWORK

3.1. System Overview

Our framework CEVAS is divided into camera-side and server-side (see Fig. 3). Agent C_i first filters the current frame F_t^i using the input filtering policy and then offloads the filtered frame \tilde{F}_t^i to the edge server. The edge server selects

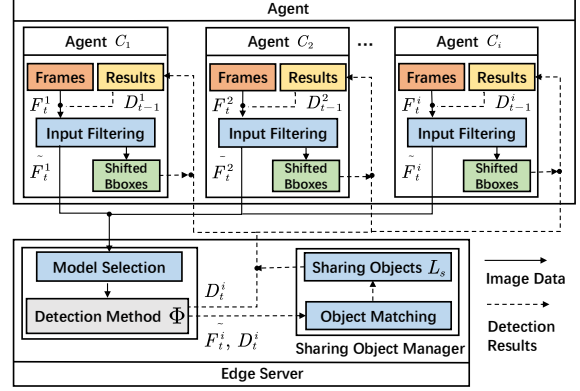


Fig. 3. The overview of our framework CEVAS.

detection methods based on the frame content, then returns the detection results D_t^i and the results of sharing objects to C_i . The sharing object manager works at the event-trigger pattern on the server side, analyzing the detection results to eliminate the spatial redundancy caused by sharing objects.

3.2. Input Filtering Policy

This section presents the fine-grained input filtering policy for producing a reasonable RoI (see Alg. 1). Different from the existing tracking-based methods [8, 9], we use the motion information obtained from optical flow to predict the appearance of new objects. Moreover, benefiting from the region partitioning policy, we only need to process part of the area on images, which significantly reduces the computation burden on the camera side. We create the queue Q_{off} and Q_r to store offloaded blocks and shifted bboxes, respectively.

For each block b_k in the incoming and leaving region, we first check if new objects appear in b_k . The number of pixels with non-zero optical flow value in b_k is set as n_k . If n_k is greater than the threshold T_{new} , we add b_k into the queue Q_{off} . Then, as for each bbox p_j in D_{t-1}^i , we calculate its motion offset x_j and y_j based on the optical flow, and use function $\Psi_{dis}(\cdot)$ to shift p_j to p'_j and obtain motion distance d_j , formulating as follows:

$$p'_j, d_j = \Psi_{dis}(p_j, x_j, y_j, f_d), \quad (1)$$

$$d_j = f_d(x_j, y_j) = \sqrt{x_j^2 + y_j^2}, \quad (2)$$

where $f_d(\cdot)$ is the function to calculate motion distance. We set a threshold T_{dis} . If $d_j > T_{dis}$, we insert the corresponding blocks of p'_j into Q_{off} . In contrast, we add p'_j into Q_r as the result of this object in the current frame since the object is probably at rest (lines 8-11 in Alg. 1). Meanwhile, if p'_j intersects with the overlapping region R_o , we also insert it into Q_{off} since we need to share its information with other agents (line 8-9 in Alg. 1). In the end, we use Q_{off} to obtain the filtered image \tilde{F}_t^i and upload \tilde{F}_t^i to the edge server.

3.3. Model Selection Policy

In this section, we design a content-aware model selection policy to enable the adaptive selection of detection methods,

Algorithm 1: Input Filtering Policy

Input : Detection results D_{t-1}^i of previous frame

- 1 Compute optical flow of current frame and create the queue Q_{off} and Q_r ;
- 2 **for** each block $b_k \in \{R_{in} \cup R_l\}$ **do**
- 3 Set the number of pixels with non-zero optical flow in b_k as n_k ;
- 4 **if** $n_k > T_{new}$ **then**
- 5 Insert b_k into Q_{off} ;
- 6 **for** each bbox $p_j \in D_{t-1}^i$ **do**
- 7 $p'_j, d_j \leftarrow$ Eq. 1;
- 8 **if** $d_j > T_{dis}$ or $(p'_j \text{ intersects with } R_o)$ **then**
- 9 Insert the corresponding blocks of p'_j into Q_{off} ;
- 10 **else**
- 11 Insert p'_j into Q_r ;
- 12 Obtain \widetilde{F}_t^i from Q_{off} and upload \widetilde{F}_t^i to the edge server;

which achieves a balance between accuracy and response latency. Let Φ denote the detection function, we can get

$$D_t^i = \Phi(\widetilde{F}_t^i). \quad (3)$$

In practice, the system can adapt to many detection methods with various characteristics and performances, for example, $\{\Phi_1, \Phi_2, \Phi_3\}$. Suppose the previous frame's results D_{t-1}^i contains the bboxes $\{p_j \mid 1 \leq j \leq N\}$, inspired by [1], we propose to calculate the average intersection over union (IoU) value of all bboxes pair in D_{t-1}^i , as follows:

$$m_{t-1}^i = \frac{N \cdot (N-1)}{2} \sum_{j=1}^{N-1} \sum_{j'=j+1}^N \Psi_{iou}(p_j, p_{j'}), \quad (4)$$

in which $\Psi_{iou}(\cdot)$ is the function to calculate the IoU between two bboxes. When m_{t-1}^i is 0, we select the fastest detection methods. Moreover, when m_{t-1}^i exceeds the threshold T_{iou} , we select the model with the largest number of parameters to achieve a higher detection accuracy. In other cases, we select those methods with moderate speed and parameter quantities.

3.4. Sharing Object Manager

We implement the sharing object manager within the edge server to update the positions of the sharing objects in overlapping region. Meanwhile, by sharing the positions of these sharing objects, our framework can ensure that each agent accurately detects the objects in their captured images. Since the previous works [1, 4] did not consider the detection accuracy of each agent while eliminating redundancy, they can not be applied in cooperative perception. The process in Alg. 2 will be triggered when obtaining the detection results D_t^i .

For each bbox p_j in D_t^i , we first check if it intersects with the overlapping region, then use the function Ψ_{feat} to obtain the corresponding object O_j and its features, as follows:

$$O_j, \chi_j^c, \chi_j^h = \Psi_{feat}(p_j, \widetilde{F}_t^i, f_c, f_h), \quad (5)$$

Algorithm 2: Sharing Object Manager

Input : Detection results D_t^i of current frame \widetilde{F}_t^i , sharing object list L_s

- 1 **for** each bbox $p_j \in D_t^i$ **do**
- 2 **if** p_i do not intersect with R_o **then**
- 3 continue;
- 4 $O_j, \chi_j^c, \chi_j^h \leftarrow$ Eq. 5;
- 5 **for** each object O_m in L_s **do**
- 6 $s_{j,m} \leftarrow$ Eq. 8;
- 7 Insert $s_{j,m}$ into the created queue Q_s ;
- 8 $s_{min} \leftarrow$ the minimum value in Q_s ;
- 9 $O_M \leftarrow$ the corresponding sharing object of s_{min} ;
- 10 **if** $s_{min} < T_s$ **then**
- 11 Update result of O_M to p_i ;
- 12 **else**
- 13 Insert O_j into the list L_s ;

where $\chi_j^c \in \mathbb{R}^{1 \times 3}$ and $\chi_j^h \in \mathbb{R}^{C \times H \times W}$ denotes the color features and image features of the object O_j , respectively. f_c and f_e denotes two feature extractors, formulating as follows:

$$\chi_j^c = f_c(p_j, \widetilde{F}_t^i; \theta_c), \chi_j^c \in \mathbb{R}^{1 \times 3}, \quad (6)$$

$$\chi_j^h = f_h(p_j, \widetilde{F}_t^i; \theta_h), \chi_j^h \in \mathbb{R}^{C \times H \times W}. \quad (7)$$

Then, we match the object O_j with the existing sharing objects in the list L_c . We obtain the distance $s_{j,m}$ between the features of O_j and O_m by

$$s_{j,m} = \sqrt{\sum_{i=1}^{N_1} (\chi_j^c(i) - \chi_m^c(i))^2} + \sqrt{\sum_{i=1}^{N_2} (\chi_j^h(i) - \chi_m^h(i))^2}. \quad (8)$$

We then insert $s_{j,m}$ into the queue Q_s . After iteration, the minimum value in Q_s is set as s_{min} , and the corresponding sharing object is O_M . If s_{min} is less than the threshold T_s , O_j is considered to be the same object with O_M , so we update the detection results of O_M to p_i . In contrast, we add O_j into L_s as a new sharing object. The results of the sharing objects in L_s will be shared among all agents.

4. PERFORMANCE EVALUATION

In this section, we conduct extensive simulations on our platform [29] to evaluate the performance of CEVAS.

4.1. Implementation Details

Simulation Settings. From *AI city challenge* dataset [30], we select a video clip of an intersection in which every four camera captures video at 10 Hz. Three variants of YOLOv5 models [31] with different speeds and accuracy are set as the corresponding detection methods. We set T_{dis} as 0.1, T_{iou} as 0.2, T_s as 0.05. T_{new} is set as a quarter of the number of pixels in a block.

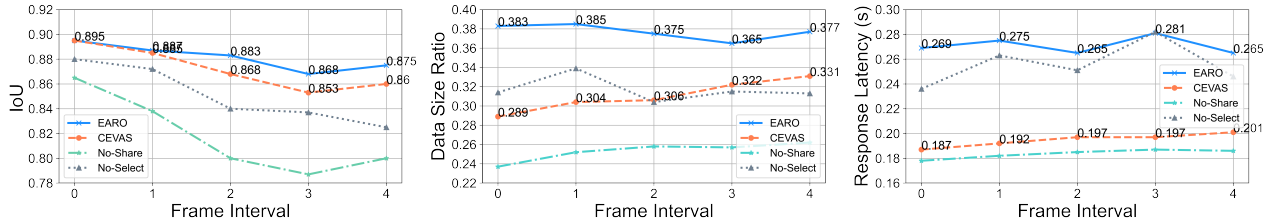


Fig. 4. Impact of Frame Interval.

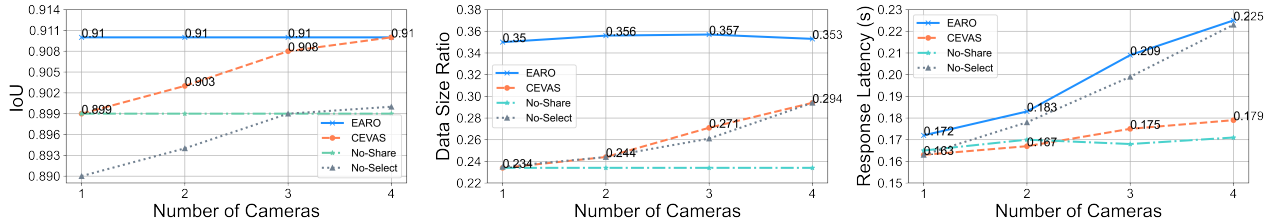


Fig. 5. Impact of the Number of Cameras.

Compared Schemes. 1) EARO [8]: EARO implements a motion vector-based object tracking mechanism to assign RoI and compress the image data of other areas. 2) No-Share: We disable the sharing object manager in this scheme, so the edge server will not share the detection results of sharing objects with other agents. 3) No-Select: This scheme is an ablation study with the model selection policy. The edge server will process the received images using a fixed detection method.

Evaluation Metrics. 1) IoU: IoU is used to evaluate the detection accuracy between the predicted bboxes and ground truth. 2) Data Size Ratio: The ratio of the amount of offloaded data to the amount of original image data. 3) Response Latency: The time consumed to detect a frame, including on-camera filtering, network transmission, and inference latency.

4.2. Impact of Frame Interval

We simulate the camera with different *fps* by setting the interval between two consecutive frames. When the frame interval is n , we pick one frame from every n frames. As shown in Fig. 4, it is apparent that CEVAS reduces the data size ratio and response latency compared to EARO, with a decrease of 18% and 28%, respectively. This indicates that our proposed input filtering policy significantly eliminates spatial and temporal redundancy, avoiding the transmission of redundant information. Moreover, CEVAS greatly reduces response latency compared with No-Select. The potential reason is that our model selection policy enables the adaptive selection of detection methods and thus increases computing efficiency. Meanwhile, CEVAS only decreases 1% in IoU compared to EARO and improves IoU by 7% and 2.5% compared to No-Share and No-Select. The above results show that CEVAS maintains high detection accuracy for each agent using fewer image data.

4.3. Impact of the Number of Cameras

To intuitively indicate our exploitation of spatial redundancy, we investigate the impact of the number of cameras. The corresponding results are shown in Fig. 5. As the number

Table 1. Impact of transmission rate on response latency.

Method	# Rate				
	80	100	120	140	160
EARO [8]	0.269	0.263	0.254	0.242	0.227
CEVAS (Ours)	0.187	0.183	0.175	0.166	0.155

of cameras increases, the methods that utilize spatial redundancy using the sharing object manager, including CEVAS and No-Select, achieve a more accurate detection, and the IoU of CEVAS gradually approaches EARO. Meanwhile, CEVAS achieves a 26% reduction in average data size ratio and 13% reduction in average response latency compared to EARO. Additionally, the response latency of EARO and No-Select without the model selection policy rises linearly with the number of cameras. In contrast, CEVAS maintains lower response latency as it avoids the unnecessary processing of redundant information and uses detection methods adaptively. From the above results, we can see that our framework can support multiple cameras and ensure scalability in large-scale environments.

4.4. Impact of Transmission Rate

Lastly, we explore the impact of the transmission rate of agents on response latency. As Table 1 shows, CEVAS reduces the response latency by 31% on average compared with EARO. It indicates that CEVAS accelerates video analytics by eliminating spatial-temporal redundancy and selecting detection methods adaptively.

5. CONCLUSION

In this paper, to achieve efficient cooperative perception, we proposed a traffic-related object detection framework CEVAS, which simultaneously eliminates the existing spatial and temporal redundancy in multi-view video data. Extensive experimental results demonstrated that our framework could considerably reduce the response latency while ensuring the detection accuracy of each agent.

6. REFERENCES

- [1] Hongpeng Guo, Shuochao Yao, Zhe Yang, Qian Zhou, and Klara Nahrstedt, “Crossroi: Cross-camera region of interest optimization for efficient real time video analytics at scale,” in *Proc. ACM MMSys*, 2021, pp. 186–199.
- [2] Yang Liu, Jing Liu, Jieyu Lin, Mengyang Zhao, and Liang Song, “Appearance-motion united auto-encoder framework for video anomaly detection,” *IEEE Transactions on Circuits and Systems II: Express Briefs*, vol. 69, no. 5, pp. 2498–2502, 2022.
- [3] Yang Liu, Jing Liu, Mengyang Zhao, Shuang Li, and Liang Song, “Collaborative normality learning framework for weakly supervised video anomaly detection,” *IEEE Transactions on Circuits and Systems II: Express Briefs*, vol. 69, no. 5, pp. 2508–2512, 2022.
- [4] Samvit Jain, Xun Zhang, Yuhao Zhou, Ganesh Ananthanarayanan, Junchen Jiang, Yuanchao Shu, Paramvir Bahl, and Joseph Gonzalez, “Spatula: Efficient cross-camera video analytics on large camera networks,” in *Proc. IEEE/ACM SEC*, 2020, pp. 110–124.
- [5] Yang Liu, Jing Liu, Mengyang Zhao, Dingkang Yang, Xiaoguang Zhu, and Liang Song, “Learning appearance-motion normality for video anomaly detection,” in *2022 IEEE International Conference on Multimedia and Expo (ICME)*. IEEE, 2022, pp. 1–6.
- [6] Dingkang Yang, Shuai Huang, Yang Liu, and Lihua Zhang, “Contextual and cross-modal interaction for multi-modal speech emotion recognition,” *IEEE Signal Processing Letters*, vol. 29, pp. 2093–2097, 2022.
- [7] Dingkang Yang, Shuai Huang, Haopeng Kuang, Yangtao Du, and Lihua Zhang, “Disentangled representation learning for multimodal emotion recognition,” in *Proceedings of the 30th ACM International Conference on Multimedia*, 2022, p. 1642–1651.
- [8] Luyang Liu, Hongyu Li, and Marco Gruteser, “Edge Assisted Real-time Object Detection for Mobile Augmented Reality,” in *Proc. ACM MobiCom*, 2019, pp. 1–16.
- [9] Yundi Guo, Beiji Zou, Ju Ren, Qingqing Liu, Deyu Zhang, and Yaoyue Zhang, “Distributed and efficient object detection via interactions among devices, edge, and cloud,” *IEEE Trans. Multimedia*, vol. 21, no. 11, pp. 2903–2915, 2019.
- [10] Huizi Mao, Taeyoung Kong, et al., “Catdet: Cascaded tracked detector for efficient object detection from video,” *Proc. MLSys*, vol. 1, pp. 201–211, 2019.
- [11] Wuyang Zhang, Zhezhi He, Luyang Liu, Zhenhua Jia, Yunxin Liu, Marco Gruteser, Dipankar Raychaudhuri, and Yanyong Zhang, “Elf: Accelerate high-resolution mobile deep vision with content-aware parallel offloading,” in *Proc. ACM MobiCom*, 2021, pp. 201–214.
- [12] Samvit Jain, Ganesh Ananthanarayanan, Junchen Jiang, Yuanchao Shu, and Joseph Gonzalez, “Scaling Video Analytics Systems to Large Camera Deployments,” in *Proc. HotMobile*, 2019, pp. 9–14.
- [13] Xiaochen Liu, Pradipta Ghosh, Oytun Ulutan, B. S. Manjunath, Kevin Chan, and Ramesh Govindan, “Caesar: Cross-camera complex activity recognition,” in *Proc. ACM SenSys*, 2019, pp. 232–244.
- [14] Kun Yang, Peng Sun, Jieyu Lin, Azzedine Boukerche, and Liang Song, “A novel distributed task scheduling framework for supporting vehicular edge intelligence,” in *2022 IEEE 42nd International Conference on Distributed Computing Systems (ICDCS)*. IEEE, 2022, pp. 972–982.
- [15] Qi Chen, Sihai Tang, Qing Yang, and Song Fu, “Cooper: Cooperative perception for connected autonomous vehicles based on 3d point clouds,” in *Proc. ICDCS*, 2019, pp. 514–524.
- [16] Tsun-Hsuan Wang, Sivabalan Manivasagam, Ming Liang, Bin Yang, Wenyan Zeng, and Raquel Urtasun, “V2vnet: Vehicle-to-vehicle communication for joint perception and prediction,” in *Proc. ECCV*, 2020, pp. 605–621.
- [17] Dingkang Yang, Shuai Huang, Shunli Wang, Yang Liu, Peng Zhai, Lizhen Su, Mingcheng Li, and Lihua Zhang, “Emotion recognition for multiple context awareness,” in *European Conference on Computer Vision*. 2022, vol. 13697, pp. 144–162, Springer.
- [18] Dingkang Yang, Haopeng Kuang, Shuai Huang, and Lihua Zhang, “Learning modality-specific and -agnostic representations for asynchronous multimodal language sequences,” in *Proceedings of the 30th ACM International Conference on Multimedia*, 2022, p. 1708–1717.
- [19] Yue Hu, Shaoheng Fang, Zixing Lei, Yiqi Zhong, and Siheng Chen, “Where2comm: Communication-efficient collaborative perception via spatial confidence maps,” *arXiv preprint arXiv:2209.12836*, 2022.
- [20] Xumiao Zhang, Anlan Zhang, Jiachen Sun, Xiao Zhu, Y. Ethan Guo, Feng Qian, and Z. Morley Mao, “Emp: Edge-assisted multi-vehicle perception,” in *Proc. ACM MobiCom*, 2021, pp. 545–558.
- [21] Hang Qiu, Po-Han Huang, Namu Asavisanu, Xiaochen Liu, Konstantinos Psounis, and Ramesh Govindan, “Autocast: Scalable infrastructure-less cooperative perception for distributed collaborative driving,” in *Proc. ACM MobiSys*, 2022, p. 128–141.
- [22] Runsheng Xu, Hao Xiang, Zhengzhong Tu, Xin Xia, Ming-Hsuan Yang, and Jiaqi Ma, “V2x-vit: Vehicle-to-everything cooperative perception with vision transformer,” *arXiv preprint arXiv:2203.10638*, 2022.
- [23] Yiming Li, Shunli Ren, Pengxiang Wu, Siheng Chen, Chen Feng, and Wenjun Zhang, “Learning distilled collaboration graph for multi-agent perception,” in *Proc. NeurIPS*, 2021, vol. 34, pp. 29541–29552.
- [24] Daniel Kang, John Emmons, Firas Abuzaid, Peter Bailis, and Matei Zaharia, “Noscope: Optimizing neural network queries over video at scale,” *Proc. VLDB Endow.*, vol. 10, no. 11, pp. 1586–1597, 2017.
- [25] Yuanqi Li, Arthi Padmanabhan, Pengzhan Zhao, Yufei Wang, Guoqing Harry Xu, and Ravi Netravali, “Reducto: On-camera filtering for resource-efficient real-time video analytics,” in *Proc. ACM SIGCOMM*, 2020, pp. 359–376.
- [26] Dingkang Yang, Yang Liu, Can Huang, Mingcheng Li, Xiao Zhao, Yuzheng Wang, Kun Yang, Yan Wang, Peng Zhai, and Lihua Zhang, “Target and source modality co-reinforcement for emotion understanding from asynchronous multimodal sequences,” *Knowledge-Based Systems*, p. 110370, 2023.
- [27] Joseph Redmon, Santosh Divvala, Ross Girshick, and Ali Farhadi, “You only look once: Unified, real-time object detection,” in *Proc. IEEE CVPR*, 2016, pp. 779–788.
- [28] Wei Liu, Dragomir Anguelov, Dumitru Erhan, Christian Szegedy, Scott Reed, Cheng-Yang Fu, and Alexander C Berg, “Ssd: Single shot multi-box detector,” in *Proc. ECCV*, 2016, pp. 21–37.
- [29] “Cevas,” <https://github.com/bruceteams/CEVAS>.
- [30] Milind Naphade, Shuo Wang, David C. Anastasiu, Zheng Tang, Ming-Ching Chang, Xiaodong Yang, Yue Yao, Liang Zheng, Pranamesh Chakraborty, Christian E. Lopez, Anuj Sharma, Qi Feng, Vitaly Ablavsky, and Stan Sclaroff, “The 5th AI City Challenge,” in *Proc. IEEE CVPRW*, 2021.
- [31] “Yolov5,” https://pytorch.org/hub/ultralytics_yolov5.